Available online at www.sciencedirect.com
SCIENCE DIRECT®
International Journal of Rock Mechanics & Mining Sciences 43 (2006) 562–571
International Journal of Rock Mechanics and Mining Sciences
www.elsevier.com/locate/ijrmms

Improved design and data interpretation of a multi-purpose borehole testing device for soft rock

Y.-W. Pan[a,*,1], J.-J. Liao[a,1], A.-B. Huang[a,1], J.-C. Chang[b,2], H.-J. Liao[b,2]

[a]Department of Civil Engineering, National Chiao Tung University, 1001 Ta Hsueh Road, Hsin-Chu, Taiwan, ROC
[b]Department of Civil Engineering, National Chiao Tung University, Hsin-Chu, Taiwan, ROC

Accepted 27 September 2005
Available online 8 November 2005

Abstract

The authors previously developed a multi-purpose borehole testing device (BTD). The purpose of the BTD was designed for obtaining mechanical properties including anisotropic elastic modulus and interface shear strength properties for soft rock that may be easily disturbed during sampling. Since the creation of the previous BTD, a few minor problems were experienced during in situ testing operation. In the present work, improvements both in equipment design and data interpretation were made. Improved design of BTD successfully reduced the chance for pressure meter test (PMT) membrane breakage, allowed larger expansion of borehole jack test (BJT), improved the waterproof of the bottom compartment and made easy for the whole equipment setup. The refined design has improved the in situ performance of BTD. New approach of data interpretation was also proposed. A series of BTD tests, including BJTs, borehole plate loading tests and borehole shear tests were carried out to demonstrate the capability of the refined borehole test device.

Keywords: Soft rock; Borehole jack test; Borehole shear test; Plate loading test; In-situ test

1. Introduction

Soft rock may be considered as a generic term covering those materials that could be described as hard clays, extremely weak rock, very weak rock and weak rock [1]. Very often, field coring can cause significant disturbance to soft rock samples and results in underestimate of material stiffness and strength [2]. Thus, the in-situ test would seem to be a more desirable alternative in characterizing the mechanical properties for soft rock. Several types of in situ borehole testing were developed for this reason such as pressuremeter test (PMT) [3], borehole jack test (BJT) [4–6], and borehole plate loading test (BPLT) [7].

Most of the borehole loading tests were designed to measure the deformability modulus of tested material adjacent to the borehole based on elasticity theory. Sometimes, test results were also attempted to estimate field strength of the material. For example, PMT results may be interpreted with plasticity theory to estimate the strength parameters [8] through best-fit. Large-sized borehole tests were also designed and carried out by Johnston et al. [9]. They developed a retrievable test rig to perform field plate-loading tests in soft rock at the bottom of a borehole, and to determine the design parameters for shallow as well as deep foundations. It has the advantage of avoiding expensive full-size foundation load tests and, yet, large enough to reflect the behavior of a rock mass that often contains defects.

The authors developed a multi-purpose in situ borehole testing device (BTD) [10] specifically for soft rock which may be easily disturbed during sampling. The development of BTD follows the basic concepts of the Goodman Jack [4] and retrievable test rig [9], but with many added capabilities. The main purpose of this device is to provide design parameters for shallow or deep foundations in soft rock. The BTD, designed to be used in a 200-mm-diameter borehole, consists of four radial curved platens at the top and a circular steel plate at the bottom. Driven by a high stress pressuremeter (PMT) and a hydraulic piston, the

*Corresponding author. Fax: +886 3 5716257.
E-mail address: ywpan@mail.nctu.edu.tw (Y.-W. Pan).
[1]Professor.
[2]Graduate Research Assistant.

1365-1609/$ - see front matter © 2005 Elsevier Ltd. All rights reserved.
doi:10.1016/j.ijrmms.2005.09.011

BTD can be used to perform BJT, borehole plate-loading test (BPLT) and borehole shear test (BST) in the same borehole. Since the original design and creation of BTD, a few minor problems were experienced during in situ testing operation, including (1) PMT membrane sometimes may break while BJT is fully unloaded, (2) the expansion stroke of BJT sometimes was not enough due to the limit of PMT's expansion strain, (3) waterproof of the bottom compartment of BTD sometimes was not satisfactory, and (4) the set-up for deformation measurement of BST was difficult to assemble and line up during the installation of BTD into a borehole. In the present work, improvements both in equipment design and data interpretation were made. This paper describes the refined design of BTD and methods of data interpretation; it also demonstrates the capabilities of BTD through a series of BTD tests.

2. Description of BTD

The new BTD is similar to the original one [10] in design, but with some improvement for durability, waterproof and measurement. The BTD consists of three major compartments as described in Fig. 1, with a total height of 1900 mm when assembled. It was designed to perform tests in a 200-mm-diameter borehole. The top compartment can be expanded laterally against the borehole wall to carry out a borehole jacking test. Also, because the lateral expansion will jam the top compartment against the borehole wall, it hence can provide reaction for the plate-loading test at the bottom of the borehole, and performs a borehole shear test against the borehole wall at the same time. The central compartment offers waterproof housing for the signal conditioning and analog/digital conversion systems. The bottom compartment serves the purpose of performing plate loading test at the bottom of the borehole. Detailed designs of these compartments are described in the following context.

2.1. Top compartment

The top compartment consists of four pieces of curved high strength aluminum platens each covering a 90° sector. When assembled and without lateral expansion, these curved platens form a hollow cylinder with an outside diameter of 200 mm, inside diameter of 76 mm and a height of 600 mm. The outside surface of the curved platens was knurled to create approximately 1-mm-deep crosshatched channels on the surface in order to roughen the platen surface.

Longitudinal holes were bored as depicted in a cross sectional view of the four curved platens as shown in Fig. 2. In the refined design of BTD, a pair of rods linked by a series of four pre-tensioned springs was used to hold the neighboring curved platens together and to retract the curved platens back to the original geometry after expansion. A high strength aluminum tube was behind the joint of each pair of neighboring curved platens to fill the opening between those neighboring curved platens after expansion. The existence of aluminum tubes would effectively reduce the potential chance of membrane breakage when the curved platens fully rebound due to unloading. The remaining space in the longitudinal holes allows the passage of hydraulic tubing and signal cables. Also in the improved design, the inner cavity of the top compartment with a diameter of 76 mm was refined in order to more closely accommodate a 74 mm diameter high stress PMT seating inside. The refined design minimizes the space between the curved platen and PMT so that allows a larger effective expansion stroke of BJT.

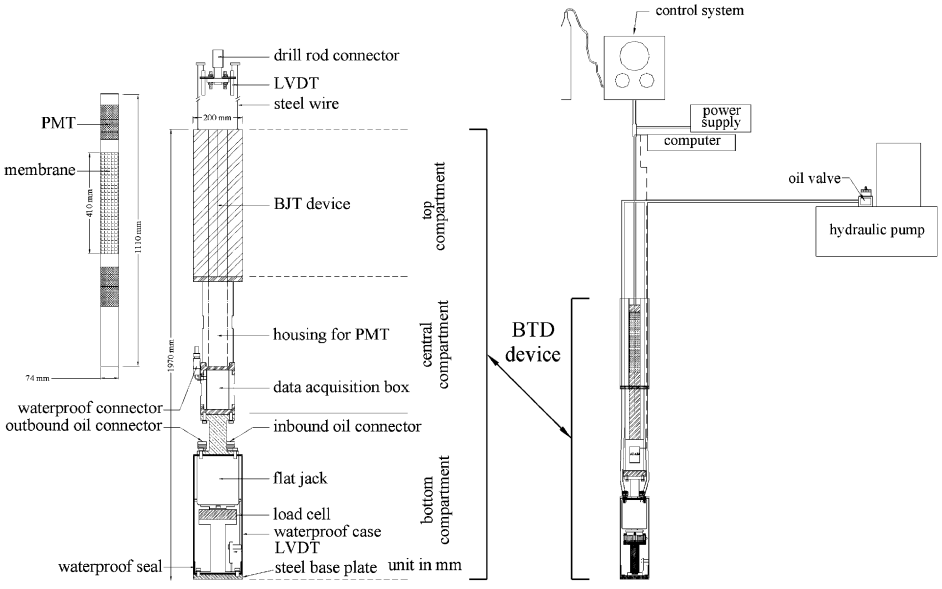

Fig. 1. Complete BTD set-up.

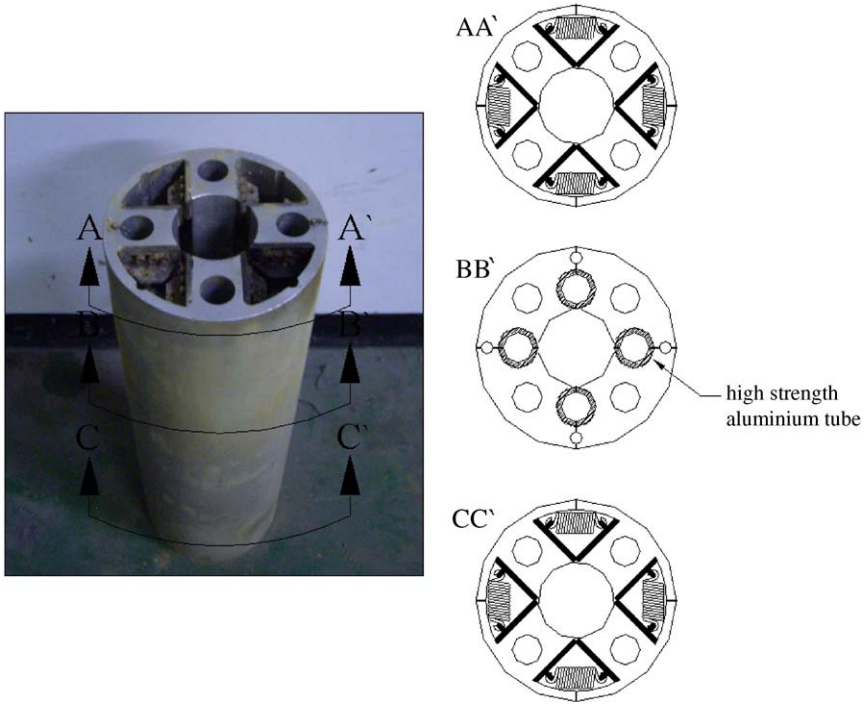

Fig. 2. Top compartment.

The PMT expansion pushes the four curved platens apart and against the wall of the borehole. The amount of radial displacement of the curved platens during expansion was monitored through the strain arms of the pressuremeter inserted in the inner cavity. The expansion of the curved platens serves as a BJT against the borehole wall. While in a BST, the compressive contact force on the borehole rock surface provides the applied normal force. During BST, a drill rod serves as the fixed reference point.

2.2. Central compartment

The central compartment, as shown in Fig. 3, transmits the longitudinal thrust between the top and bottom compartments. The main component of the central compartment was a thick-walled waterproof cylindrical container. A signal conditioning board and an analog/digital converter system were housed in the container. All analog signals (one load cell and four LVDT's) were fetched into the central compartment and converted into digital forms before passing to the ground surface. This arrangement minimizes signal/noise and the number of wires required in the system. The central compartment separates the circular plate of the bottom compartment from the top compartment by approximately 1300 mm or 6.5 times the diameter of BTD. This separation assures minimum interference between the top and bottom compartments created by their individual movements.

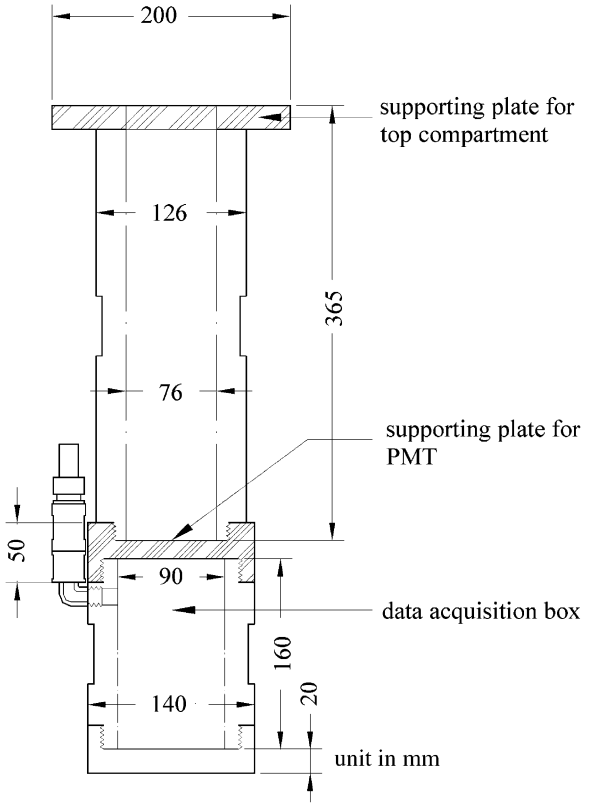

Fig. 3. Central compartment.

2.3. Bottom compartment

The bottom compartment, shown in Fig. 4, consists of a 300 kN thrust capacity, 50 mm stroke hydraulic piston. The

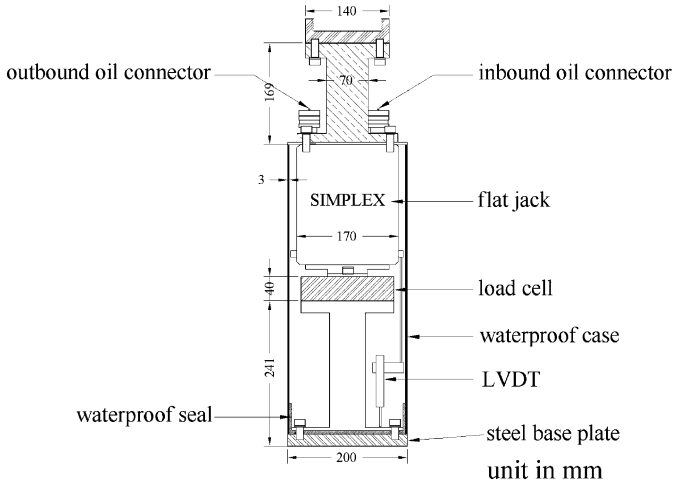

Fig. 4. Bottom compartment.

piston was used to push a 20 mm thick, 200 mm diameter base plate against the bottom of the borehole. Movement of the base plate was monitored by an LVDT. A load cell was placed immediately below the hydraulic piston to monitor the axial force during the plate-loading test. The bottom compartment was sealed in a steel casing for waterproofing.

2.4. High-stress pressuremeter

A high-stress PMT was developed specifically for soft rocks and to work as a component of the BTD. The expandable portion of the pressuremeter probe had a diameter of 74 mm and a length of 410 mm. The PMT was equipped with 12 strain arms distributed in three levels; at each level, four strain arms were distributed evenly on the circular plane (separated by 90°) so that can measure the lateral expansion along two mutually perpendicular directions at each level. Details of the PMT were described in a previous paper [10].

3. Methods of borehole tests with BTD

3.1. Borehole preparation

To minimize disturbance, a multi-step borehole preparation procedure was made. An NX-sized core barrel with water circulation was used to advance the borehole to a depth 0.3 m above the designated depth where the bottom of the BTD was to be seated. The existing borehole was then enlarged with a HX core barrel, 170 mm diameter reamer, 200 mm diameter fishtail reamer, in sequence. The borehole was further enlarged using 220 mm diameter reamer down to a depth 2 m above the designated depth to ease the later retrieval of BTD after borehole test. Subsequently, the borehole was advanced again using a 200 mm diameter reamer to a depth 100 mm above the designated depth where the bottom of the BTD was to be seated. Finally, to assure borehole verticality and minimum accumulation of loose material at the bottom, a 200 mm diameter core barrel was used to advance the last 100 mm depth of the borehole. The BTD occupied approximately the bottom 2 m of the borehole. All drilling fluid was completely pumped out after boring.

The fully assembled BTD with the pressuremeter inserted in the top compartment, was lowered to the bottom of the borehole. The BTD was suspended using a tripod/pulley mechanism and a steel cable. Upon seating of the BTD, the tension in the steel cable was released and the tripod moved aside. A drill rod serves as the fixed reference point in the borehole test. Two pre-tensioned steel wires link the head of the top compartment and LVDT fixed to a fixed end plate connecting to the drill rod as illustrated in the upper-left portion of Fig. 1. The LVDT was responsible for picking up the shear displacement during BST.

3.2. BTD test procedure

A full set of BTD tests includes BJT, BPLT and BST. The first step in a BTD test was to perform a BJT by expanding the top compartment against the borehole wall through pressuremeter inflation. The next step was to perform the BPLT to the bottom of the borehole using the bottom compartment, and concurrently the BST to the borehole wall using the top compartment. During the BPLT and BST, the maximum lateral expansion pressure applied in the BJT remained constant. Upon completing BPLT/BST, the pressures applied at top and bottom compartments were completely released and the BTD reseated. For the BTD tests reported herein, at least three sets of BPLT/BST tests were carried out at each tested section in a borehole, each with a different maximum contact pressure applied to the borehole wall through the top compartment. Details of the test procedure are described as follows.

3.2.1. Expansion of the top compartment—BJT

The pressuremeter inside of the top compartment was expanded stress-controlled in 98 kPa increments. When the expansion pressure exceeded 980 kPa, the increment was changed to 196 kPa. The duration for each increment was 60 s. The pressuremeter expansion pushes the curved platens against the borehole wall and performs a BJT. For each BJT, pressure was first gradually increased, and unloading/reloading cycles were carried out in three different pressure levels (in some case, the third unloading/reloading cycle was not possible because the PMT had reached its maximum radial strain level before reach the third pressure level). Finally, the pressure was fully released.

3.2.2. BPLT and BST

The PMT pressure p_e in the top compartment results in a contact normal stress p_i applied to the borehole wall. A series of load increments was applied in a BPLT test. For

each load increment, the applied load remained constant until the plate settlement stabilized. This usually took approximately 2 min for each increment. The same applied load pushed the top compartment upward and performed a BST against the borehole wall. The BPLT was terminated when the hydraulic piston of the bottom compartment reached its maximum stroke, the applied load reached 220 kN (capacity of the load cell) or the top compartment reached its maximum shearing resistance and started moving. The BST is a result of action and reaction between the top and bottom compartments of the BTD. After the BPLT and BST, the pressure applied to the hydraulic piston and the pressuremeter was completely released to allow retraction of the curved platens and the hydraulic piston.

4. Methods of data interpretation

4.1. Calibration of the BTD

In the BJT, the top compartment was driven by the high-stress pressuremeter. The pressuremeter was calibrated first to establish the membrane stiffness and compliance of the pressuremeter system.

The four pieces of curved platens were linked together through a series of springs as described earlier. The friction of these linkage mechanisms and stiffness of the springs as well as the friction between the top and the central compartments created resistance when the top compartment was expanded. This system stiffness referred to as k_{cp} was calibrated by expanding the top compartment with its pressuremeter inserted in the internal cavity. The fully assembled top compartment was suspended in the air using a cable then performs an expansion test without any restriction from the outside of the top compartment. Results of the PMT pressure (p_e) versus radial strain (i.e., the ratio of diameter change, $\Delta D/D$) of the top compartment are shown in Fig. 5. The value of p_i was calculated from the PMT pressure with adjustments for membrane stiffness and system compliance of PMT. Three different linear segments were noted. For radial strain below 2.6%, PMT had not yet touched the set of curved platens, the slope k_{cp} (the slope of p_e versus ΔD) was 0.026 MPa/mm primarily due to the PMT's stiffness. Within 2.6% and 3.8%, k_{cp} was 0.043 MPa/mm possibly contributed by PMT's stiffness and the static friction between the top and the central compartments. Beyond 3.8%, k_{cp} was 0.012 MPa/mm possibly contributed by PMT's stiffness and the dynamic friction between the top and the central compartments.

In addition, the compressibility of the PMT membrane was also calibrated by loading the PMT inside the top compartment against a thick rigid steel tube with an inner diameter 205 mm. Through calibration, the required correction for membrane compliance was 0.008 MPa/mm.

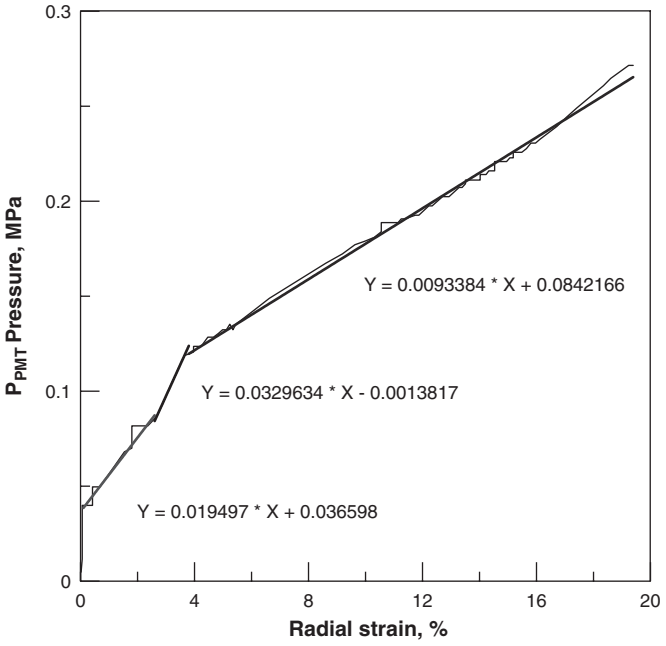

Fig. 5. Calibrated results of PMT pressure versus radial strain of the top compartment.

4.2. Data interpretation for BJT

During BJT, the PMT expands and pushes four curved platens against the rock surrounding the borehole. To model the mechanics of the loaded curved platen, a series of two-dimensional numerical simulation of the BJT by computer code *FLAC* were conducted to determine the contact pressure acted by curved platen against the surface of borehole loaded through the PMT pressure. The surrounding rock was modeled as a non-associated Mohr–Coulomb material with a variety of combinations of material properties including Young's modulus, shear modulus, cohesion, friction angle and dilation angle for typical soft rock. In the BJT simulation, a uniform inner pressure (representing the pressure acted by the PMT onto the curved platen) was applied on a rigid curved block representing the curved platen; the rigid curved block was initially in contact with the rock material surrounding a borehole (200 mm). The simulation assumed that the interface between the quarter ring and the rock material behaved as a discontinuity with strength parameters equals to two-thirds of the strength of rock material. The calculated curve of contact pressure versus deformation of BJT simulation was compared with the pressure-deformation curve of the expansion of a 200 mm cavity.

Fig. 6 shows the typical calculated pressure–deformation curves for both BJT and PMT for the same borehole. The pressure–deformation curve is dependent on the material constants. The difference in the pressure–deformation curves of BJT and PMT resulted from the difference in the two problems' different boundary conditions, pressure distribution and the shear stress transfer on the interface. It was found that the ratio of pressures corresponding to any

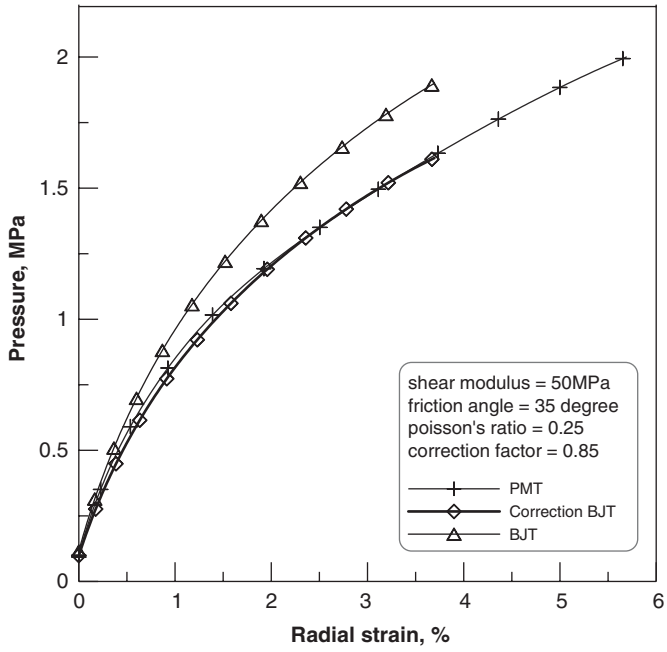

Fig. 6. Typical calculated pressure–deformation curves for BJT and PMT.

deformation is generally close to 0.85, regardless of the change in material parameters. As a result, $\alpha = 0.85$ was used as the correction factor in directly applying the cavity expansion theory for the interpretation of BJT result. Furthermore, an additional correction factor $\beta = 0.86$ is applied to take into account three-dimensional effect [4]. The shear modulus is estimated using the ratio of the corrected contact normal stress, p_i, and the expansion deformation of BJT on the basis of the cavity expansion theory. Thus, the shear modulus, G_{BJ} can be computed using the relationship between theq change of contact normal stress (Δp_i) on the borehole and the diameter change of the top compartment (ΔD) as follows:

$$G_{BJ} = \alpha\beta D\frac{\Delta p_i}{\Delta D}, \tag{1}$$

where D is the borehole diameter. Corrections of the net internal expansion pressure should be made for the system stiffness and membrane compliance. The net internal expansion pressure is $(p_i - \int k_{cp}\Delta D)$ in which the value of k_{cp} should be determined according to the calibration curve as shown in Fig. 5 and ΔD.

The PMT pressure, p_e, can be multiplied by a correction factor $\gamma = 0.24$ to obtain the equivalent cavity pressure p_i. The ratio 0.24 comes from the ratio of the pressured perimeter area of actual PMT probe ($D = 76$ mm, $L = 410$ mm) and that of perimeter area of the BJT ($D = 200$ mm, $L = 600$ mm). Using p_e instead of p_i, the shear modulus can be obtained by

$$G_{BJ} = \alpha\beta\gamma D\frac{\Delta p_e}{\Delta D}. \tag{2}$$

4.3. Data interpretation of BPLT

The BPLT generates a load-displacement (Q_p–δ) curve in the vertical direction. This load–displacement curve may be used to determine a Young's modulus in the vertical direction (E_z) as [7]

$$E_z = \frac{Q_p}{\delta D_p}(1 - \upsilon^2)\mu_o, \tag{3}$$

where D_p—diameter of the plate, which was 200 mm, υ—Poisson's ratio, and μ_o—the depth correction factor.

A υ value of 0.4 was chosen based on P–S logging data at depths comparable to BPLT (bottom of the borehole). According to Pells [7], the given υ and dimensions of the BTD, a μ_o of 0.38 was used for Eq. (6).

5. Demonstrated field borehole tests with BTD

5.1. BTD tests in soft rock

A series of field tests has been carried out in a soft rock formation at a test site in Hsinchu County, which was located in central northern Taiwan. The outcrop of the test site contains Pleistocene poorly cemented massive sandstone formation. The orientation of the formation has its strike N48°E and dip angle 29°. Three 5 m boreholes numbered B-1, B-2 and B-3, were drilled at the test site. The rock cores were used to conduct laboratory tests. However, due to difficulties in sampling, the obtained rock cores were not necessarily suitable for mechanical property testing. For each borehole test, the PMT was carefully oriented to let two sets of PMT strain arms be parallel and perpendicular, respectively, to the strike of rock formation. Two sets of BJT, BPLT and BST using BTD were performed in each borehole at two different depth levels: BJT/BST were conducted at the depths 0.5–1.1 and 3.5–4.1 m; BPLT were conducted at the depths 2.5 and 5.5 m.

5.2. Results of BTD tests

5.2.1. BJT

Figs. 7 and 8 show the typical curves of internal expansion pressure, p_i versus radial strain in a BJT. Fig. 7 is the pressure versus radial strain along the strike direction, while Fig. 8 is the pressure versus radial strain along the dip direction. The slopes of the unloading/reloading curves were used to determine the shear modulus of rock surrounding the borehole at various pressure levels and along different directions. The PMT pressure was multiplied by a correction factor $\gamma = 0.24$ to account for the ratio of the pressured perimeter area of PMT and PJT. The shear modulus was obtained using Eq. (2).

The ΔD values were the average of the pressuremeter strain arm readings. Table 1 lists the shear moduli obtained for all BJTs along both the strike direction and the dip direction. For each borehole, two BJTs were conducted in

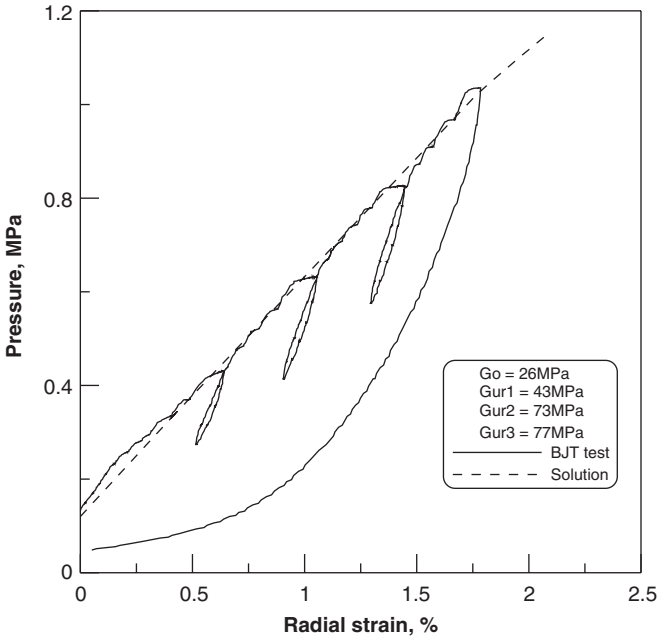

Fig. 7. Pressure versus radial strain along the strike direction in a BJT.

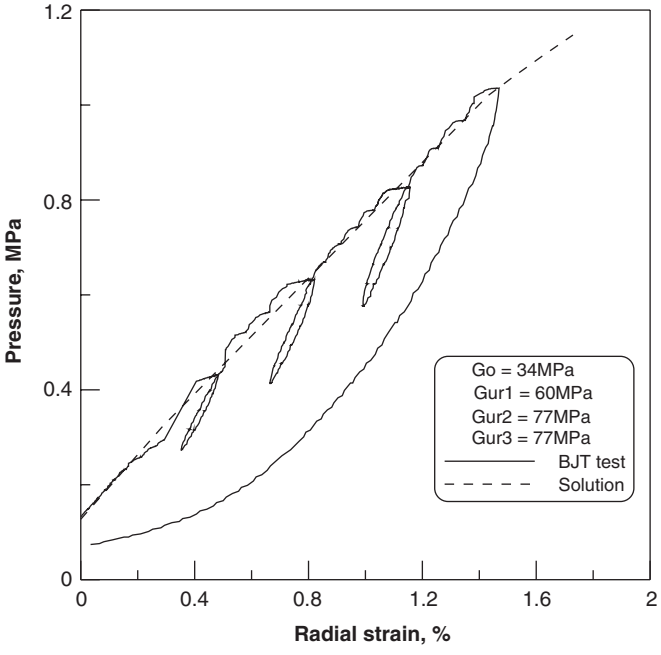

Fig. 8. Pressure versus radial strain along the dip direction in a BJT.

each borehole at two different depth levels (0.5–1.1 and 3.5–4.1 m). In Table 1, G_o denotes the shear modulus of the initial portion of the loading curve, G_{ur1}, G_{ur2} and G_{ur3}, respectively, denote the shear moduli obtained for the 1st, the 2nd and the 3rd unloading/reloading cycles.

The BJT results clearly demonstrate several interesting features. First, the unloading/reloading modulus is at least twice larger than the modulus of the initial loading portion. Next, the unloading/reloading shear modulus increases as the tested depth increases. Also, the modulus corresponding to a larger unloaded pressure level appears slightly higher possibly because of crack-closure effect. The cycles of expanding the top compartment may also have a stiffening effect on the surrounding material. One more very interesting feature is that the shear modulus along the dip direction appears consistently larger than that along the strike direction.

Table 1
Shear moduli obtained from BJT along various directions

Test no.	Direction	G_o (MPa)	G_{ur1} (MPa)	G_{ur2} (MPa)	G_{ur3} (MPa)
0420J	Strike	10	27	28	—
	Dip direction	11	40	48	—
0423J	Strike	26	43	73	77
	Dip direction	34	60	77	77
0426J	Strike	17	37	62	100
	Dip direction	18	45	120	88
0428J	Strike	11	21	26	—
	Dip direction	14	32	40	—
0429J	Strike	12	28	39	—
	Dip direction	16	36	43	—
0430J	Strike	10	18	26	—
	Dip direction	20	36	43	—

The combination of material stiffening and slight variations in the borehole diameter was the main reason for the variation in the measured stiffness. Nevertheless, measured shear moduli at a same depth appear reasonably close. *P–S* logging tests were carried out in a nearby borehole, the shear modulus at the depths 1 and 4 m were 93.3 and 147.6 MPa, respectively. It appeared the modulus obtained by BJT was smaller than the modulus obtained from *P–S* logging. This is, however, not surprising since the modulus from *P–S* logging represents modulus at much smaller strain level than those under BJT loading.

5.2.2. BPLT and BST

Figs. 9–11 demonstrate the relationship between the respective displacements measured at top and bottom compartments and applied load for the BPLT and BST performed in borehole B-1, under three different normal pressure levels. Each set of BPLT/BST was conducted under a constant normal stress between the curved platen and surrounding rock in the BJT. For the test, the vertical displacement of BST was according to the LVDT readings taken at the end of drill rod. Two steel wires connecting the top compartment and the drill-rod end enabled the determination of the relative shear displacement of the top compartment during BST. The vertical displacement of BPLT was calculated as the LVDT measurements at the bottom compartment minus those from top of the top compartment.

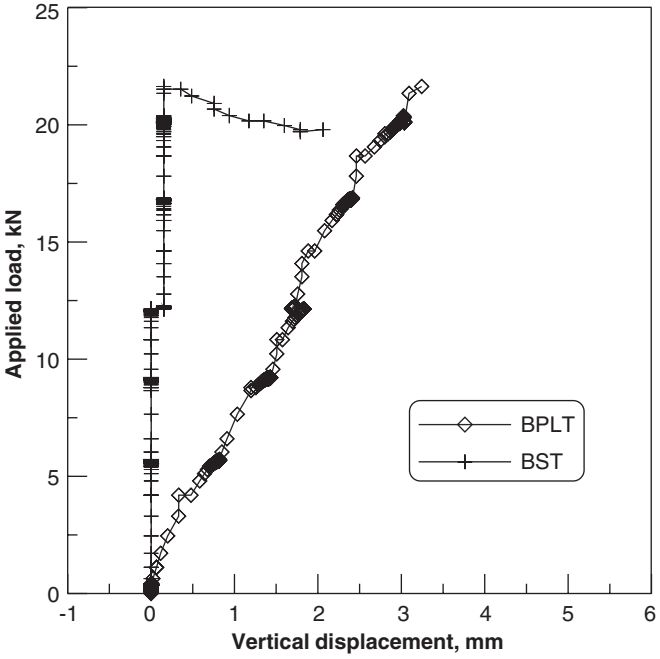

Fig. 9. Applied load versus displacement for BPLT and BST under BJT contact pressure 0.11 MPa.

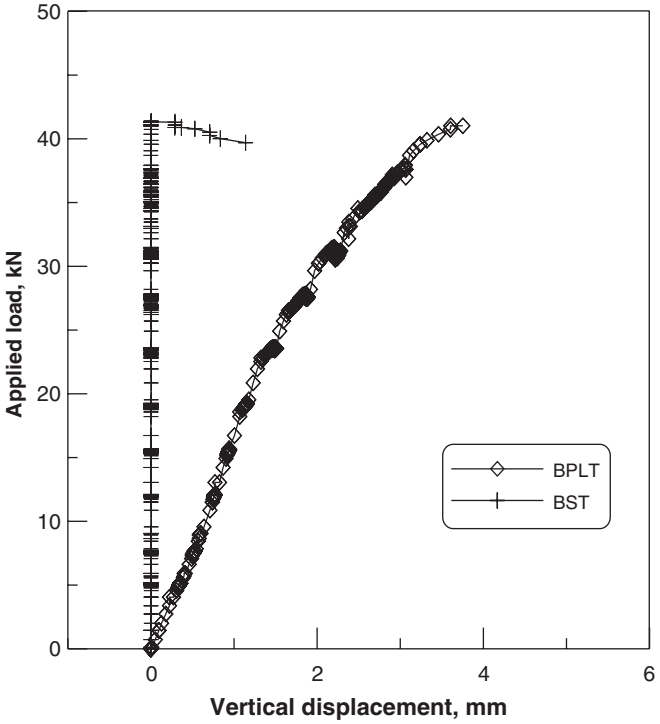

Fig. 10. Applied load versus displacement for BPLT and BST under BJT contact pressure 0.19 MPa.

In Figs. 9–11, the curves with diamond symbol are the vertical load versus vertical displacement in BPLT. Figs. 8–10, respectively, present results of BPLT and BST for contact normal pressure between BJT's curved platen and rock equal to 0.11, 0.19 and 0.26 MPa, respectively. Fig. 10,

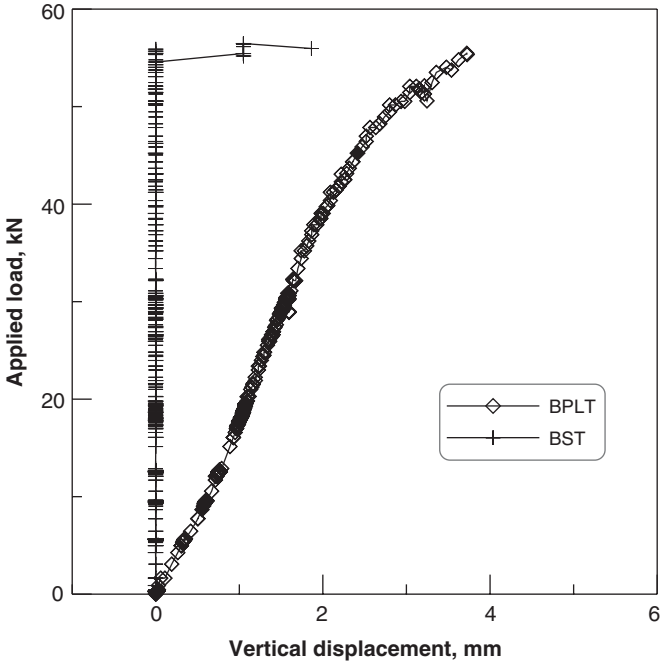

Fig. 11. Applied load versus displacement for BPLT and BST under BJT contact pressure 0.26 MPa.

e.g., a Young's modulus 46.3 MPa in the vertical direction can be determined from the slope of the linear portion in the BPLT load-displacement curve using Eq. (3). This modulus represents the Young's modulus in the vertical direction. Based on the results of *P*–*S* logging tests near the tested site, the Poisson's ratio ν was about 0.4. The corresponding shear modulus can also be estimated. The applied normal pressure was raised in each sequence of BPLT/BST tests. Series 0428, e.g., BPLT/BST tests under three different normal pressures 110, 188 and 263 kPa were conducted in sequence. The Young's modulus obtained was found somewhat increased for a BPLT with a previous loading in BPLT. For example, the three Young's moduli from three subsequent BPLTs are 23.4, 46.3 and 53 MPa, sequentially. The increase of modulus with preloading may be resulted from the densification of the material underlying the loading plate.

Also in Figs. 9–11, the curve with plus symbols is the shear force against the shear displacement in BST. The maximum vertical load from BPLT is also the maximum shear resistance offered by the top compartment. The curve demonstrates clearly that shear slip would not occur before the shear force reached a yielding force (in this case 41.5 kN). The maximum vertical load divided by the surface area of the top compartment represents the peak shear stress (τ_{max}) in the BST. Fig. 10, e.g., the yielding shear force resulted in a peak shear stress τ_{max} of 105 kPa on the perimeter of sheared BST rock interface. A series of BPLT/BST was conducted at three normal stress levels at a same depth in a borehole. The yielding shear stress could be plotted against the normal stress applied on the interface to obtain the failure envelope as shown in Fig. 12. The

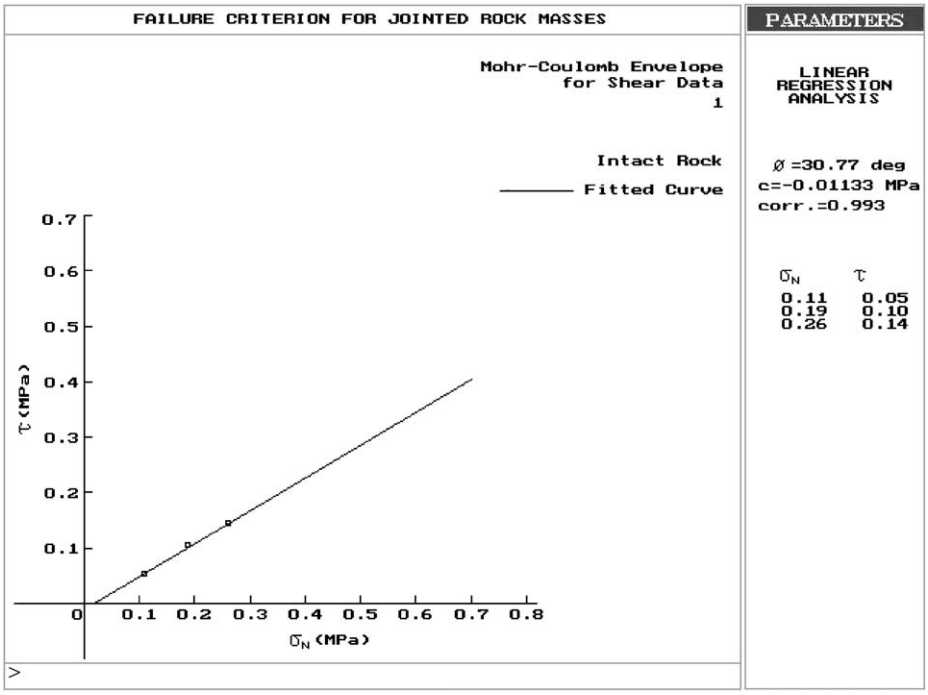

Fig. 12. Envelope of interface strength.

friction angle from the BST's represents the interface strength between the surrounding soft rock and the knurled aluminum platens. In the illustrated test series, an interface friction angle of 31° was obtained without any cohesion. For comparison, the dry soft rock has a friction angle 50° and a cohesion 0.7 MPa, from laboratory triaxial tests.

6. Summary and conclusions

A multi-purpose in situ borehole testing device (BTD) previously developed by the authors was refined in its design and data interpretation. The purpose of the BTD was specifically for obtaining mechanical properties including anisotropic elastic modulus and interface shear strength properties for soft rock that may be easily disturbed during sampling. Since the creation of the previous BTD, a few minor imperfections in design were experienced during in situ testing operation. Improvement in the design of BTD successfully reduced the chance for PMT membrane breakage allowed larger expansion of BJT, improved the waterproof of the bottom compartment and made easy for the whole equipment setup. The refined design has improved the in situ performance of BTD.

Numerical simulation was conducted to model the mechanics of BJT in order to determine the contact pressure acted by curved platen against the borehole surface during BJT. From the numerical simulation, it was found that the contact pressure could be related to a factored cavity expansion pressure corresponding to a same deformation with a same size of borehole. The shear modulus was then estimated using the ratio of corrected contact pressure and expansion deformation of BJT on the basis of cavity expansion theory. Corrections of the net internal expansion pressure were made for the system stiffness, membrane compliance, and three-dimensional effects.

A series of BTD tests, including BJT, BPLT and BST, was carried out to demonstrate the capability of the refined borehole test device. From each BJT, shear modulus along two perpendicular horizontal directions could be obtained from two sets of deformation measurement in PMT. From BPLT, the Young's modulus along the vertical direction was determined. From BST, the shear strength on the rock interface could be determined. The results obtained from these tests appeared consistent and compatible with laboratory results and other field tests. The BTD may serve as a good tool for providing the stiffness and interface strength of soft rock for shallow or deep foundations in soft rock.

Acknowledgement

The research project was funded by the National Science Council of ROC.

References

[1] Johnston IW. Soft rock engineering. In: Comprehensive rock engineering: principles, practice, and projects, vol. 1: fundamental. 1993; p. 367–93.

[2] Tatsuoka F, Kohata Y. Stiffness of hard soils and soft rock in engineering applications. In: Mitachi Shibuya, Balkema Miura, editors. Proceedings of the first international symposium on pre-failure deformation of geomaterials. Japan: Sapporo; 1995. p. 947–1066.

[3] Rocha M, da Silveira A, Grossmann N, de Oliveira E. Determination of the deformability of rock masses along borehole. Proceedings of the first ISRM conference, vol. 1. 1966; p. 697–704.
[4] Goodman RE, Van TK, Heuze FE. Measurement of rock deformability in boreholes. Proceedings of the tenth US symposium on rock mechanics, Austin TX. 1968; p. 523–55.
[5] Amadei B. The influence of rock mass fracturing on the measurement of deformability by borehole expansion tests. Proceedings of the 26th US symposium on rock mechanics. 1985; p. 859–67.
[6] Amadei B, Valverde M, Jernigan R, Touseull J, Cappelle JF. The directional dilatometer: a new option to determine rock mass deformability. In: Ballivy, editor. The pressuremeter and its new avenues. Rotterdam: Balkema; 1995. p. 257–64.
[7] Pells PJN. Plate loading tests on soil and rock. In situ testing for geotechnical investigations. Rotterdam: Balkema; 1983. p. 73–86.
[8] Haberfield CM, Johnston IW. The interpretation of pressuremeter tests in weak rock—theoretical analysis. Proceedings of the third international symposium on pressuremeter. Oxford, Telford, London. 1990; p. 169–78.
[9] Johnston IW, Donald IB, Bennet AG, Edwards JW. The testing of large diameter pile rock sockets with a retrievable test rig. Proceedings of the third Australia–New Zealand conference on geomechanics, Wellington. vol. 1, 1980; p. 105–8.
[10] Huang AB, Fang CK, Liao JJ, Pan YW. Development of a multipurpose borehole testing device for soft rock. J Geotech Test 2002;25(3):83–90.